ORIGINAL ARTICLE

european journal
of neurology
the official journal of the european academy of neurology

Brain connectivity abnormalities and treatment-induced restorations in patients with cervical dystonia

Liang Feng[1] | Dazhi Yin[2,3] | Xiangbin Wang[4] | Yifei Xu[1] | Yongsheng Xiang[4] | Fei Teng[1] | Yougui Pan[1] | Xiaolong Zhang[1] | Junhui Su[1] | Zheng Wang[3,5] | Lingjing Jin[1] ⓘ

[1]Neurotoxin Research Center of Key Laboratory of Spine and Spinal Cord Injury Repair and Regeneration of Ministry of Education, Department of Neurology, Tongji Hospital, Tongji University School of Medicine, Shanghai, China

[2]Key Laboratory of Brain Functional Genomics (MOE and STCSM), Institute of Cognitive Neuroscience, School of Psychology and Cognitive Science, East China Normal University, Shanghai, China

[3]Institute of Neuroscience, CAS Center for Excellence in Brain Science and Intelligence Technology, Chinese Academy of Sciences, Shanghai, China

[4]Department of Radiology, Tongji Hospital, Tongji University School of Medicine, Shanghai, China

[5]University of Chinese Academy of Sciences, Beijing, China

Correspondence
Lingjing Jin, Neurotoxin Research Center of Key Laboratory of Spine and Spinal Cord Injury Repair and Regeneration of Ministry of Education, Neurological Department of Tongji Hospital, Tongji University School of Medicine, 389 Xincun Road, Shanghai, 200065, China.
Email: lingjingjin@163.com

Zheng Wang, Institute of Neuroscience, Chinese Academy of Sciences, 320 Yueyang Road, Shanghai, 200031, China.
Email: zheng.wang@ion.ac.cn

Abstract

Background: The relationship between brain abnormalities and phenotypic characteristics in cervical dystonia (CD) patients has not been fully established, and little is known about the neuroplastic changes induced by botulinum toxin type A (BoNT-A) treatment.

Methods: Ninety-two CD patients presenting with rotational torticollis and 45 healthy controls from our database were retrospectively screened. After clinical assessment, the 92 patients underwent baseline magnetic resonance imaging (MRI) followed by a single-dose injection of BoNT-A. Four weeks later, 76 out of the 92 patients were re-evaluated with the Tsui scale for dystonia severity, and 33 out of 76 patients completed post-treatment MRI scanning. Data-driven global brain connectivity and regional homogeneity in tandem with seed-based connectivity analyses were used to examine the functional abnormalities in CD and longitudinal circuit alterations that scaled with clinical response to BoNT-A. Multiple regression models were employed for the prediction analysis of treatment efficacy.

Results: Cervical dystonia patients exhibited elevated baseline connectivity of the right postcentral gyrus with the left dorsomedial prefrontal cortex and right caudate nucleus, which was associated with their symptom severity. BoNT-A reduced excessive functional connectivity between the sensorimotor cortex and right superior frontal gyrus, which was significantly correlated with changes in Tsui score. Moreover, pre-treatment regional homogeneity of the left middle frontal gyrus was linearly related to varied response to treatment.

Conclusions: Our findings unravel dissociable connectivity of the sensorimotor cortex underlying the pathology of CD and central effects of BoNT-A therapy. Furthermore, baseline regional homogeneity with the left middle frontal gyrus may represent a potential evidence-based marker of patient stratification for BoNT-A therapy in CD.

Liang Feng and Dazhi Yin contributed equally to the paper.

INTRODUCTION

Cervical dystonia (CD) is the most common form of focal dystonia [1]. Primary clinical manifestations include intermittent or persistent posture abnormalities and movement disorders of the head and neck, accompanied by neck pain and tremor [2]. CD patients are usually classified into one of four types: torticollis, laterocollis, retrocollis, anterocollis, depending on the abnormal posture of head and neck. Torticollis involves head and neck rotation and constitutes more than half of CD cases [3]. Patients often suffer gradually worsening symptoms throughout the course of the disease [4], which severely affect their quality of life. Accumulating neuroimaging evidence has demonstrated maladaptive changes in brain regions responsible for sensorimotor control, including the motor areas and basal ganglia [5], the primary and secondary somatosensory cortices [6,7] and even the occipital lobe, in CD patients [8]. Beyond these focal brain abnormalities, the disrupted neural circuit integration hypothesis is becoming a leading pathophysiological model for CD [9], particularly for functional connectivity derived from resting-state functional magnetic resonance imaging (fMRI) data. Graph theoretical analysis has shown altered topological organization of the basal ganglia, sensorimotor network and default mode network [10]. Using independent component analysis, Delnooz and colleagues reported aberrant within-network connectivity of the sensorimotor, visual and executive control networks [11] and between-network connectivity of the basal ganglia with the left fronto-parietal and sensorimotor networks [12]. However, given the substantial heterogeneity in patients with CD, associations between brain abnormalities and phenotypic characteristics have not been fully established [13].

Dystonia symptoms can be alleviated by a variety of procedures, including focal injection of botulinum toxin type A (BoNT-A) [3], transcranial magnetic stimulation [14], deep brain stimulation [15] and performing the sensory trick in which dystonic contractions are improved temporarily by touching the body segment [16]. Focal injection of BoNT-A as a first-line choice of treatment can selectively block targeted neuromuscular junctions resulting in biochemical denervation of the treated muscles [17]. Recent evidence suggests that BoNT-A injection to the dystonic neck muscles may trigger a cascade of modulatory effects in the brain [18]. Pioneering task-based fMRI studies have consistently reported that effective BoNT-A therapy would either increase activation of the secondary somatosensory cortex, insular and inferior parietal lobule [19,20] or reduce activation of the supplementary motor area and dorsal premotor cortex [21] in CD patients. Furthermore, recent studies using resting-state

fMRI demonstrated that BoNT-A treatment resulted in not only partial restoration of functional dysconnectivity in the basal ganglia, the sensorimotor and primary visual networks [11,22], but also active regulation of connectivity between the frontal areas with the right mid-ventral striatum and external globus pallidus [12]. Despite considerable progress, it remains unclear whether the neuroplastic modulation of brain circuits triggered by BoNT-A therapy is causally associated with symptomatic improvement and how it is attributable to varied clinical response in CD patients [23].

To address these questions, a large cohort of CD patients with a particular focus on rotational torticollis were screened from our database, which has the highest prevalence. A data-driven approach, voxel-wise global brain connectivity (GBC) and regional homogeneity (ReHo) in tandem with seed-based connectivity analysis, were deployed to detect brain-wide functional abnormalities in CD patients relative to healthy controls (HCs) and associations with their clinical symptoms. The aim of our study was to investigate the neural mechanism in CD patients, identify core regions where the neuroplastic changes caused by BoNT-A treatment occur in the brain connectivity network, and ascertain whether they can be used as supplementary judgments for the clinical outcome of BoNT-A therapy in individuals. It was hypothesized that the functional connectivity of the sensory-motor integrative network may be disrupted in CD patients, some of which could be normalized after clinical symptoms were reduced by BoNT-A treatment. In addition, the clinical efficacy of BoNT-A therapy could be determined by abnormalities of specific regions in this network before treatment.

METHODS

Participants

Ninety-two CD patients and 45 HCs between December 2016 and November 2019 were screened from our institutional database. Inclusion criteria were as follows: (i) idiopathic CD of which the dominant feature was rotational torticollis; (ii) right-handedness; (iii) course of illness longer than 1 month; (iv) no history of BoNT-A treatment within the past 6 months; (v) no history of surgical operation for CD; (vi) no medical history of physical or psychiatric disorders, except for dystonia; (vii) patients not taking antispasmodic or psychoactive drugs within 4 weeks before BoNT-A treatment; (viii) no abnormalities in routine MRI head scan. The exclusion criteria were (i) severe head tremor; (ii) dystonia beyond the cervical region;

(iii) pregnant and lactating women; (iv) alcohol or drug abuse. This study was approved by the ethical committee of Shanghai Tongji Hospital, Tongji University School of Medicine, and all participants voluntarily provided written informed consent.

All patients underwent clinical evaluation: the Tsui scale was used to assess dystonia severity by a neurologist and the Diagnostic and Statistical Manual of Mental Disorders (DSM-5) was used to diagnose psychiatric disorders by a psychiatrist. The patients with psychiatric conditions were not included in our study. After the neck muscles were examined by single-photon emission computed tomography [24] and other means, the patient underwent fMRI scan and then was treated with BoNT-A (Botox, Allergan Plc, Ireland/Hengli, Lanzhou Institute of Biological Products Co.Ltd, China) in concentrations of 25 IU/ml. Four weeks after treatment, 33 out of 92 patients had a second fMRI scan and Tsui scale assessment; the others failed to return to hospital. Amongst those who failed to return, 43 patients were visited in their homes and completed the Tsui scale re-evaluation only. A detailed scheme of this study is shown in Figure 1. The patients did not take antispasmodic or psychoactive drugs within 4 weeks after BoNT-A treatment.

## Magnetic resonance imaging acquisitions and preprocessing

Magnetic resonance images were acquired on a Siemens MAGNETOM Trio 3.0 T MRI scanner (Siemens, Erlangen, Germany) at the Department of Radiology of Tongji Hospital, including high-resolution T1-weighted images, T2-weighted images and resting-state fMRI data. The details of the scanning and preprocessing protocols can be found in Appendix S1 and in our previous studies [25–27]. Subjects whose head motion was >3 mm in translation or >3° in rotation were excluded. In addition, the mean displacement of micro head motion as a covariate in the following statistical analyses was considered. To further evaluate the potential effects of micro head motion, many validation analyses were performed. See Appendix S1 for more details.

Voxel-wise GBC and ReHo analysis

After preprocessing, a data-driven voxel-wise GBC analysis [28] was performed that examines connectivity from a given voxel (or area) to all other voxels (or areas) simultaneously by computing average connectivity strength—thereby producing an unbiased approach to the location of global dysconnectivity. Here, the GBC within a brain mask derived from the Automated Anatomical Labeling (AAL) atlas (90 brain areas) was computed. Furthermore, absolute correlation values were used to calculate the GBC, which represents the global connectivity strength of each voxel. To average the GBC map across subjects, GBC values were normalized across the brain using a z-standardized approach:

$$z\text{GBC}_i = \frac{\text{GBC}_i - M}{\sigma}$$
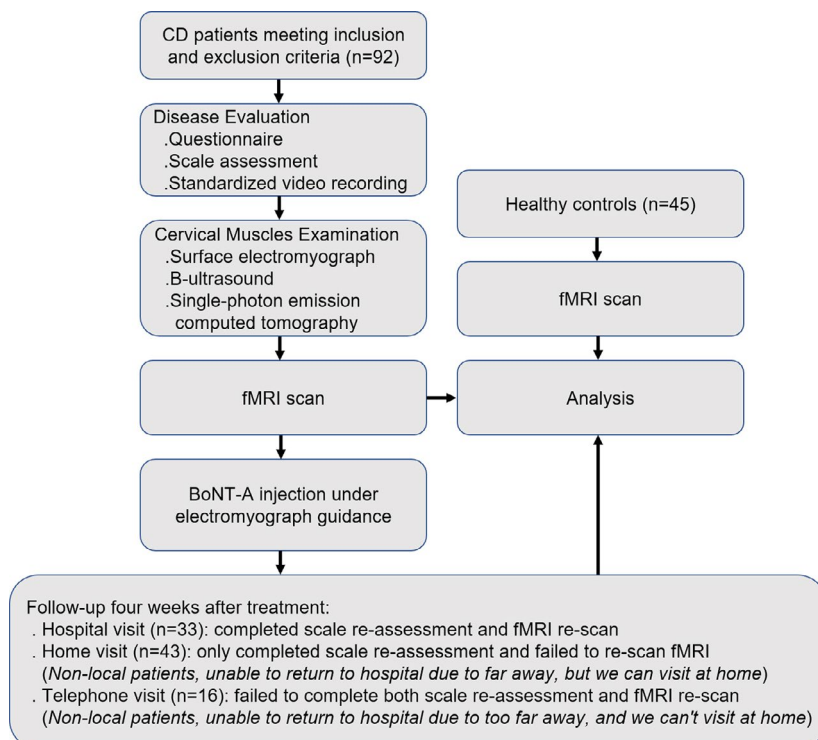
FIGURE 1 Experimental procedures. The flow chart shows the experimental procedure of the study. BoNT-A, botulinum toxin type A; CD, cervical dystonia; fMRI, functional magnetic resonance imaging [Colour figure can be viewed at wileyonlinelibrary.com]

where GBC_i denotes the GBC value of the ith voxel, M indicates the mean value of GBC across the brain mask and σ indicates the standard deviation of GBC within the brain mask.

To investigate the characteristic of local synchronization, the ReHo analysis was performed based on Kendall's coefficient of concordance. ReHo measures the similarity of the time series at a given voxel to the time series of its 26 nearest neighbors. For standardization purposes, each individual ReHo map was divided by its own mean ReHo of that entire brain. Notably, the calculation of ReHo is based on the preprocessed images without smoothing. Instead, the smoothing (full-width at half maximum 6 mm) was conducted on the ReHo map. More details can be found in our previous study [29].

Seed-based functional connectivity analysis

To further pin down changes in specific region-wise connectivity, the regions with altered GBC or ReHo in CD patients were selected as regions of interest for the seed-based functional connectivity analysis. A two-tailed one-sample t test was conducted for the HC and CD groups ($p < 0.05$, AlphaSim corrected with a voxel-level $p < 0.0001$). The within-group functional connectivity patterns of HC and CD patients were then overlapped together to generate a mask. To restrict the comparison within the relevant network only, between-group statistical analysis was finally conducted within the above created mask.

Statistical analysis

Demographic and clinical data were expressed as the mean ± SD and were analyzed using the Pearson chi-squared test, Mann–Whitney U test or Wilcoxon signed-rank test, where appropriate.

Differences between CD patients and HCs in terms of GBC, ReHo and functional connectivity measures were evaluated by two-tailed, two-sample t tests with age, sex, education and mean head motion as covariates. Correction for multiple comparisons was further conducted using an AlphaSim program which was determined by 1000 Monte Carlo simulations (i.e., single voxel $p < 0.001$, combining a minimum cluster size). Thus, a corrected $p < 0.05$ was considered as statistically significant. For the regions of interest that were identified with altered GBC, ReHo or functional connectivity values, paired t tests were conducted for patients before and after treatment, and two-sample t tests were conducted for group comparison of patients with head rotation to right and left. These subgroups of patients were also compared with HCs. Considering three times of comparisons here, a Bonferroni method was therefore used to correct it and considered $p < 0.05/3$ as statistically significant.

Pearson or Spearman correlation analysis was used to examine the relationship between abnormal GBC, ReHo and seed-based functional connectivity and clinical variables (Tsui scores and duration of illness) in CD groups. Moreover, the relationship between longitudinal alterations in GBC/ReHo/functional connectivity and treatment outcomes (delta Tsui scores) was examined.

A multiple regression analysis was performed between voxel-wise GBC and ReHo at baseline and delta Tsui scores, with age, sex, education, mean head motion and disease duration as covariates. For this brain-wide statistical analysis, multiple comparisons correction was also conducted using an AlphaSim program which was determined by 1000 Monte Carlo simulations (i.e., single voxel $p < 0.001$, combining a minimum cluster size). Post hoc Pearson correlation analysis was performed between pre-treatment GBC and ReHo of identified brain regions and changes in Tsui score after treatment. $p < 0.05$ was considered statistically significant.

RESULTS

Clinical characteristics and treatment outcome

Magnetic resonance imaging data from 14 pre-treatment patients, one post-treatment patient and one healthy control were excluded due to excessive motion during MRI scanning. Hence, 78 patients were included in subsequent analyses. Data from 62 patients with scale reassessment were used for prediction analysis of treatment efficacy, and data from 30 out of 62 patients with post-treatment imaging data were used for treatment effect analysis.

There were no significant differences in gender, age or years of education between CD patients and HCs. Tsui scores of 62 patients and 30 patients respectively 4 weeks after treatment were significantly lower than those before treatment (Table 1). This demonstrates that symptoms of CD patients were significantly improved after BoNT-A therapy.

Altered GBC, ReHo and functional connectivity between CD patients and HCs at baseline

Between-group analysis showed that CD patients exhibited significantly decreased GBC in the right superior frontal gyrus (SFG) and left dorsomedial prefrontal cortex (DMPFC), and reduced ReHo in the right inferior temporal gyrus (ITG) and bilateral postcentral gyrus (PostCG) compared to HCs (Figure 2a and Table 2). Based on the right SFG seed, CD patients showed significantly increased connectivity with the bilateral calcarine, bilateral PostCG and right precentral gyrus, and decreased connectivity with the right angular gyrus. Compared to HCs, elevated connectivity of the left DMPFC with three clusters including the bilateral fusiform gyrus and right PostCG and decreased connectivity with the dorsal anterior cingulate cortex were observed in patients. Moreover, reduced connectivity was found between the right ITG and regions including the left fusiform gyrus and inferior occipital gyrus, and increased connectivity was found between the right ITG and regions including the bilateral DMPFC and right inferior frontal gyrus. In addition, decreased connectivity of the left PostCG with two clusters including the bilateral paracentral lobule and right precentral gyrus, stronger connectivity of the right PostCG with two clusters including the bilateral thalamus and right caudate nucleus, and decreased connectivity with the bilateral precentral gyrus and left cuneus were

Clinical variables	CD (n = 78)	HCs (n = 44)	p value
Male	28	13	0.476
Age (years)	46.24 ± 12.93	46.11 ± 14.69	0.936
Education (years)	10.62 ± 4.10	10.61 ± 5.77	0.979
Disease duration (months)	34.19 ± 35.61	–	–
Tsui score	9.55 ± 3.29	–	–
Subgroups	Pre-treatment	Post-treatment	p value
Tsui score[a]	9.60 ± 3.59	4.87 ± 3.40	p < 0.001
Tsui score[b]	9.55 ± 3.38	4.55 ± 3.17	p < 0.001

Abbreviations: CD, cervical dystonia; HCs, healthy controls.

[a]Patients with both post-treatment imaging data and clinical scores were used for treatment effect analysis (n = 30).

[b]Patients with post-treatment clinical scores were used for prediction analysis of treatment efficacy (n = 62).

observed (Figure 2b and Table 2). The details of within-group analysis are shown in (Figures S1–S3). No significant changes in the above results were observed between CD patients with head rotation to right and left (Figures S4–S7).

Restored GBC, ReHo and functional connectivity for CD patients after BoNT-A treatment

After BoNT-A injection, CD patients showed significantly increased GBC in the right SFG and ReHo in the bilateral PostCG. No significant difference in GBC of the right SFG and ReHo of bilateral PostCG was observed between CD patients after treatment and HCs (Figure 3a,b). Compared to pre-treatment, connectivity strength between the right SFG and regions including the bilateral PostCG and right precentral gyrus was dramatically lower and connectivity strength between the right PostCG and right precentral gyrus was significantly higher in CD patients after treatment. There were no significant differences in these four connectivities between CD patients after treatment and HCs (Figure 3c).

Relationships between GBC/ReHo/functional connectivity and clinical variables

Baseline correlation analysis showed that both functional connectivity of the left DMPFC with the right PostCG and functional connectivity of the right PostCG with the right caudate nucleus were positively correlated with Tsui score (r = 0.30, p = 0.007; r = 0.24, p = 0.035; Figure 2c). No correlation was found between the functional connectivity and illness duration. Moreover, no significant correlations were revealed between GBC/ReHo and clinical variables. Meanwhile, significant positive correlations were observed between altered connectivity of the right SFG with the bilateral PostCG (r = 0.36, p = 0.049; r = 0.41, p = 0.024) and the right

precentral gyrus (r = 0.59, p = 0.0006) and changes in Tsui score (Figure 3d).

## Prediction of treatment efficacy based on GBC/ReHo at baseline

Multiple regression analysis revealed that the ReHo of the left middle frontal gyrus at baseline was able to significantly predict changes in the Tsui score of CD patients after treatment (Figure 4a,c). No correlation was found between the GBC at baseline and changes in Tsui score. Specifically, the ReHo of the left middle frontal gyrus at baseline was positively correlated with changes in Tsui score (r = 0.372, p = 0.003, Figure 4b).

Note that the potential effects of head motion during MRI scanning to the functional connectivity analysis were carefully examined and the present main results remained essentially unchanged (Figures S8–S10).

DISCUSSION

Previous task-related and resting-state fMRI studies have suggested the basal ganglia involvement in focal dystonia [10,12,20,22]. Increased activation in the caudate nucleus was observed when CD patients performed a forearm contraction task [30]. Some diffusion tensor imaging studies have also revealed altered microstructure in the caudate nucleus of CD patients [31,32], speculating that the caudate nucleus may be particularly relevant to CD because it has consistently been linked to head turning in stimulation studies [31]. Moreover, a theoretical framework has been proposed that altered subcortical gating of sensory information in the thalamus might induce an overload of sensory information reaching the cortex, thus leading to dysfunction of the somatosensory cortex in focal dystonia [33]. Specifically,
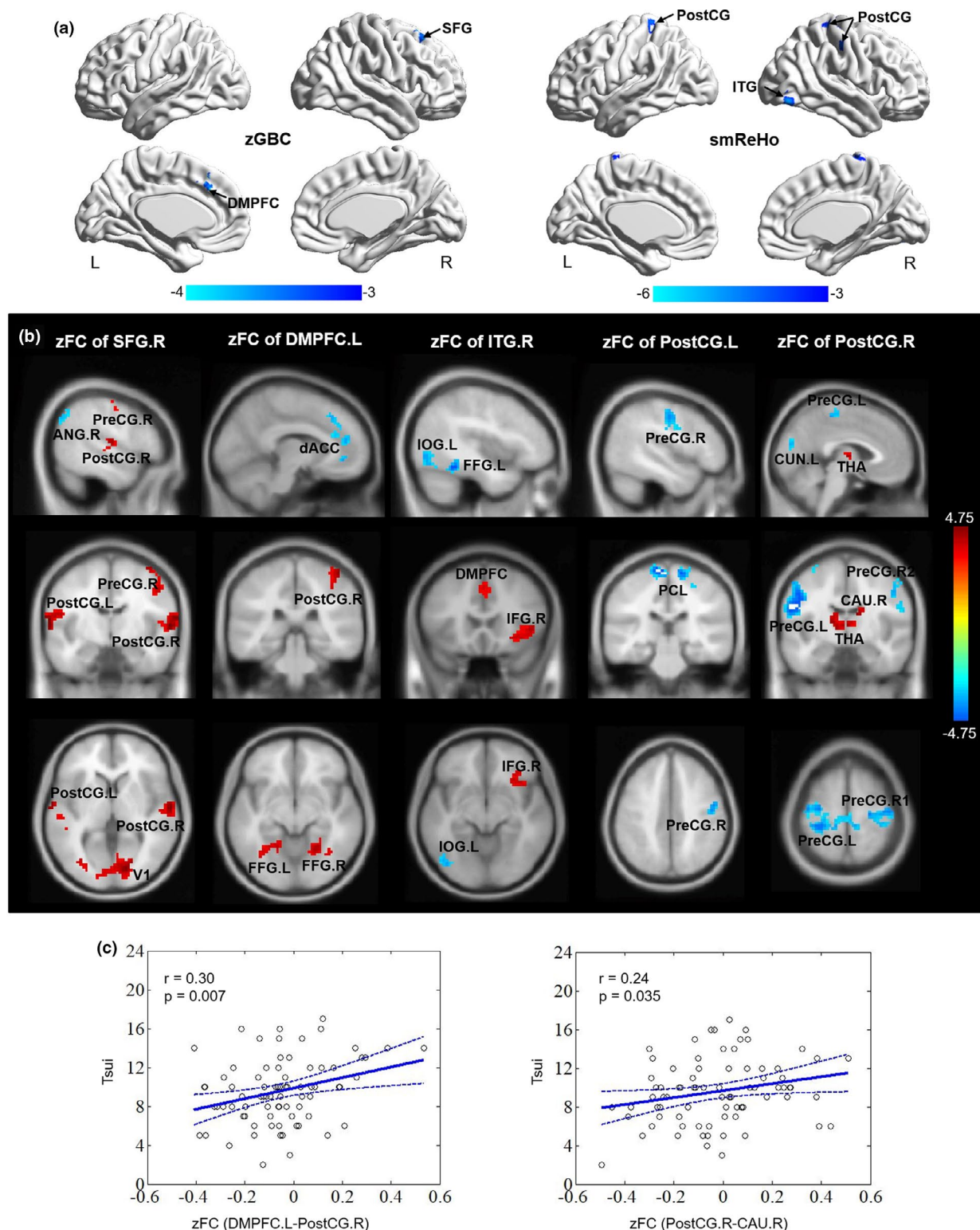
dysfunction of the PostCG has been heavily implicated in the underlying pathological circuit model of CD [10,34–36], even in those non-idiopathic cases that are acquired secondary to focal brain lesions [6]. Also the DMPFC, mainly involving the pre-supplementary motor area, is known as a core element of the sensorimotor network [11], whereby the DMPFC–PostCG–caudate nucleus connectivity may act as a key functional pathway for neck motor control. Nevertheless, relative to HCs, alterations of

connectivity with the visual cortex, dorsal anterior cingulate cortex, right angular gyrus, left cuneus and thalamus were found but not in association with clinical characteristics. Although abnormal activity in bilateral occipital cortices and thalamus has been reported previously [8,11,20,22,30], no sequential changes in the occipital cortex and thalamus caused by BoNT-A injection were identified. This observation, independent of symptom severity or treatment outcome, is likely to indicate a collateral role of the

FIGURE 2 Altered global brain connectivity, regional homogeneity and functional connectivity in cervical dystonia patients. (a) Patients exhibited significantly (left panel) decreased global brain connectivity (zGBC) in the right superior frontal gyrus (SFG) and left dorsomedial prefrontal cortex (DMPFC) and (right panel) reduced regional homogeneity (smReHo) in the right inferior temporal gyrus (ITG) and bilateral postcentral gyrus (PostCG) compared to healthy controls. Color bars indicate t values. (b) Using the right superior frontal gyrus (SFG.R) as a seed, its connected brain regions where functional connectivities significantly differed in patients and healthy controls were plotted in a column (the left hand side). Similarly, using the left dorsomedial prefrontal cortex (DMPFC.L), right inferior temporal gyrus (ITG.R), left postcentral gyrus (PostCG.L) and right postcentral gyrus (PostCG.R) as individual seeds, all brain regions with significant difference between patients and healthy controls were plotted in columns. For between-group comparisons, $p < 0.05$, AlphaSim corrected with voxel-level $p < 0.001$. Warm and cold colors indicate positive and negative connectivity, respectively. Color bars indicate t values. (c) Both the functional connectivity of left DMPFC with right PostCG and the functional connectivity of right PostCG with right caudate nucleus (CAU.R) were positively correlated with Tsui scores in patients. Dashed lines indicate 95% confidence intervals. ANG.R, right angular gyrus; CUN.L, left cuneus; dACC, dorsal anterior cingulate cortex; FFG.L, left fusiform gyrus; FFG.R, right fusiform gyrus; IFG.R, right inferior frontal gyrus; IOG.L, left inferior occipital gyrus; PCL, paracentral lobule; PreCG.L, left precentral gyrus; PreCG.R, right precentral gyrus; THA, thalamus; V1, bilateral calcarine; zFC, functional connectivity [Colour figure can be viewed at wileyonlinelibrary.com]

visual cortex and thalamus in the etiology and therapeutics of CD. Taken together, these findings collectively point to a sensorimotor circuit model which maladaptively processes information integration between sensory input and motor output, and may contribute to the core pathophysiology of CD [37,38].

Partial normalization of disrupted functional connectivity in the sensory-motor integrative network was observed in patients after a single-dose injection of BoNT-A into the dystonic neck muscles, and in particular the extent of decrease in excessive functional connectivity between right SFG (i.e., premotor cortex) and sensorimotor cortex was correlated with symptom improvement. Although previous studies have observed functional modulation of the secondary somatosensory, inferior parietal cortices, supplementary motor area and dorsal premotor cortex in CD patients after treatment [19–21], the present finding provides a direct link between BoNT-induced changes in connectivity of the sensorimotor network and reduced symptom severity. Interestingly, Sarasso and colleagues reported that the connectivity of the primary sensorimotor area was reduced in CD patients during the sensory trick execution, and the improvement of dystonic posture was correlated with a decrease in functional connectivity between precentral gyrus and PostCG/SFG [16]. It is plausible to hypothesize that different intervention means may achieve comparable therapeutic outcomes by targeting the same pathway like the SFG–sensorimotor connection. Using a low-frequency therapeutic paradigm of repetitive transcranial magnetic stimulation, a recent randomized study tested the therapeutic efficacy of four cortical regions as stimulation targets and found that targeting the dorsal premotor and primary motor cortical areas led to better treatment outcome compared to supplementary motor area and anterior cingulate cortex [14]. Although reduced baseline connectivity of the anterior cingulate gyrus with DMPFC was observed, consistent with prior reports [6,16,35], neither its relation to clinical symptoms nor longitudinal changes following BoNT-A treatment were identified. This may explain why the anterior cingulate cortex was not an optimal stimulation target for treating CD [14].

Notably, it was found that the ReHo of the left middle frontal gyrus at baseline was positively correlated with changes in Tsui score after BoNT-A therapy whilst no significant difference in ReHo was observed in the left middle frontal gyrus between HCs and CD patients before treatment. Meanwhile, Opavský and colleagues found

that CD patients showed overactivity in the contralateral secondary somatosensory cortex compared to controls, and BoNT-A treatment led to reduced activation of the ipsilateral supplementary motor area and dorsal premotor cortex in patients [21]. These observed divergences may hint that different neural circuits may underlie the pathological and therapeutic processes in CD patients. Such circuit divergence for pathology and treatment was also demonstrated in other diseased brain conditions [39].

Some limitations of the present study should be taken into account when interpreting our findings. First, the main objective here is to investigate the therapeutic effects of BoNT-A such that CD patients who received other treatments were not recruited, which definitely merits future investigation to compare treatment efficacy and outcome of BoNT-A with other therapies. Meanwhile, MRI examination was not performed repeatedly after 4 weeks for HCs such that some random effects were not strictly controlled. Secondly, the Tsui scale was used to evaluate the symptom severity of individual patients before and after treatment, which is indispensably susceptible to the rater's bias. Hence some objective measures like cervical range of motion assessed with magnetic-inertial sensors [16] can be used as a supplementary means in future experimental design. Thirdly, although the cerebellum has been known to play an important role in the pathophysiology of dystonia [40], it was not completely covered in some subjects using the present MRI scanning protocol (balancing the tradeoff between scan time and motion artifact). Thus, this study mainly focused on the central effects of BoNT-A in the cortical and basal ganglia areas that have been predominantly reported by prior studies [19–21]. In the future, a faster MRI acquisition sequence (i.e., multiband echo planar imaging sequence) can be used to acquire more brain slices for larger spatial coverage within a shorter MRI scan time.

Taken together, dissociable DMPFC–PostCG–caudate nucleus and SFG–sensorimotor connectivity pathways in tight association with neuropathology and BoNT-A treatment central effects for CD patients were identified. Investigating pre-treatment fMRI-derived parameters may contribute to the identification of predictive imaging-based biomarkers, which further help to screen candidate CD patients who may benefit most from BoNT-A injection, if validated with prospective testing.

TABLE 2 Altered GBC, ReHo and brain connectivity in CD patients compared with HCs

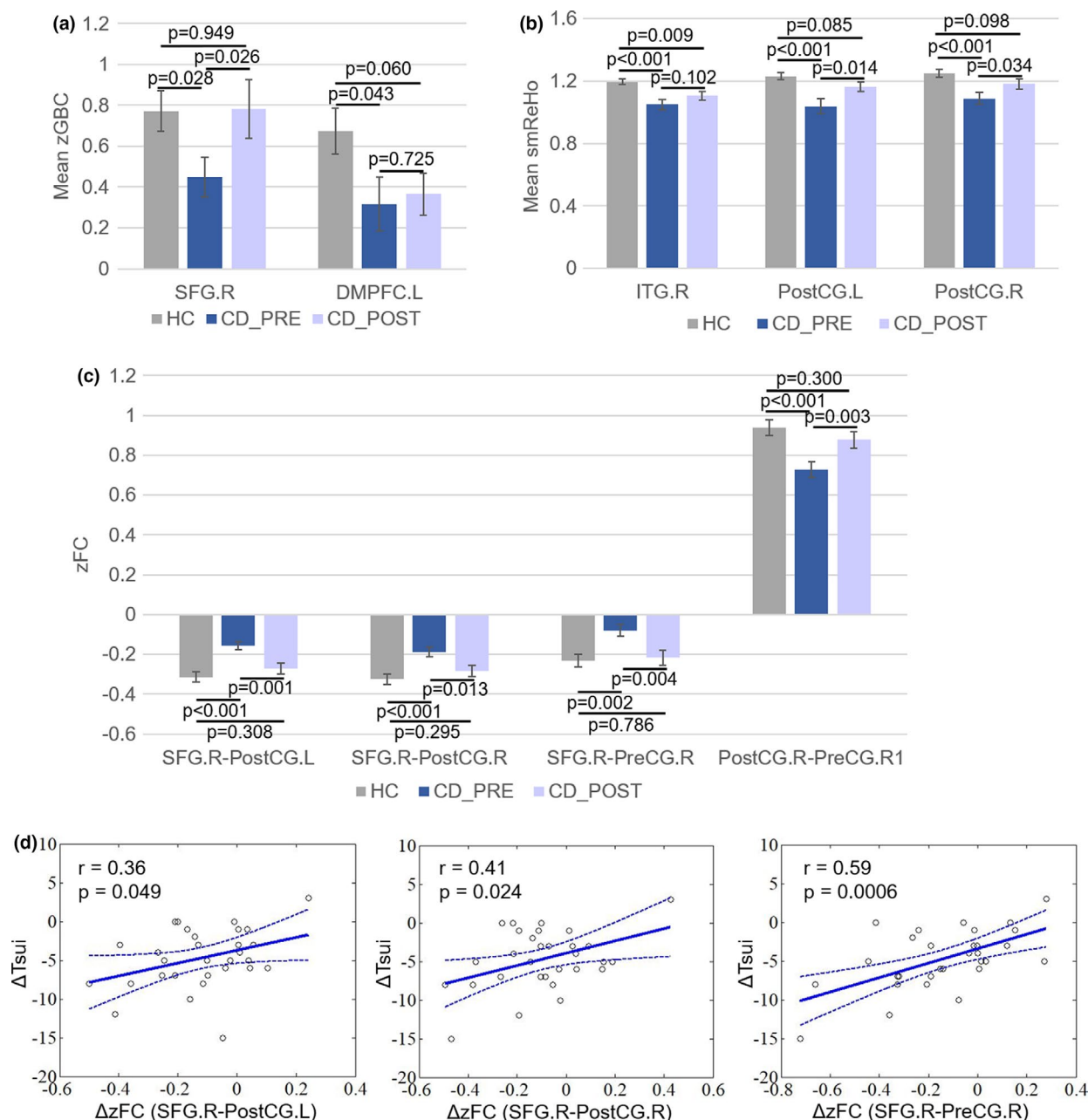| Regions	Brodmann areas	Peak MNI coordinates			Peak t scores	Cluster sizes
		x	y	z		
GBC analysis						
SFG.R	BA8	21	21	60	−3.8804	46
DMPFC.L	BA9	−3	30	36	−3.9466	31
ReHo analysis						
ITG.R	BA37	45	−54	−18	−5.0392	142
PostCG.R	BA3	51	−18	45	−4.9661	185
PostCG.L	BA3	−18	−36	66	−4.6494	159
Brain connectivity analysis						
DMPFC.L (seed)						
FFG.L	BA19	−15	−63	0	4.4894	107
FFG.R	BA19	21	−57	−9	4.1754	99
dACC	BA32	0	27	39	−4.5011	206
PostCG.R	BA1	45	−33	63	4.2498	46
SFG.R (seed)						
Visual	BA17	15	−87	−3	4.8114	330
PostCG.L	BA43	−63	−9	6	4.9893	165
PostCG.R	BA43	63	−15	9	5.5187	192
ANG.R	BA39	48	−72	42	−4.2846	52
PreCG.R	BA4,6	42	−9	66	4.1246	61
ITG.R (seed)						
DMPFC	BA32	0	21	42	3.6843	44
FFG.L	BA37	−45	−48	−18	−4.707	44
IFG.R	BA47	48	27	6	4.7694	105
IOG.L	BA18–19	−45	−72	−6	−3.882	61
PostCG.L (seed)						
PCL	BA6	−6	−27	69	−5.6228	287
PreCG.R	BA4,6	51	−6	42	−4.2773	75
PostCG.R (seed)						
CAU.R	–	12	−9	18	4.4019	40
CUN.L	BA18	−6	−81	24	−3.7588	32
PreCG.L	BA4,6	−51	−12	27	−5.3314	762
PreCG.R1	BA4,6	42	−18	66	−4.862	196
PreCG.R2	BA4,6	63	3	30	−4.4976	131
THA	–	0	−12	6	4.4777	75

Abbreviations: ANG.R, right angular gyrus; CAU.R, right caudate nucleus; CD, cervical dystonia; CUN.L, left cuneus; dACC, dorsal anterior cingulate cortex; DMPFC.L, left dorsomedial prefrontal cortex; FFG.L, left fusiform gyrus; FFG.R, right fusiform gyrus; GBC, global brain connectivity; HCs, healthy controls; IFG.R, right inferior frontal gyrus; IOG.L, left inferior occipital gyrus; ITG.R, right inferior temporal gyrus; MNI, Montreal Neurological Institute; PCL, paracentral lobule; PostCG.L, left postcentral gyrus; PostCG.R, right postcentral gyrus; PreCG.L, left precentral gyrus; PreCG.R, right precentral gyrus; ReHo, regional homogeneity; SFG.R, right superior frontal gyrus; THA, thalamus; Visual, bilateral calcarine.

FIGURE 3 Global brain connectivity, regional homogeneity and functional connectivity are restored in cervical dystonia patients after a single-dose injection of botulinum toxin type A. (a) Mean standardized global brain connectivity (zGBC) values for the right superior frontal gyrus (SFG.R) and left dorsomedial prefrontal cortex (DMPFC.L) are shown across the three groups; cervical dystonia (CD) patients before treatment (CD_PRE), CD patients after treatment (CD_POST) and healthy controls. Error bars denote SEM. (b) Mean regional homogeneity (smReHo) values for the right inferior temporal gyrus (ITG.R), left postcentral gyrus (PostCG.L) and right postcentral gyrus (PostCG.R) across groups are shown. Error bars denote SEM. (c) Mean strength of functional connectivity (zFC) of the SFG.R with the PostCG.R, PostCG.L, right precentral gyrus (PreCG.R) and mean strength of zFC between the PostCG.R and the PreCG.R1 across groups are shown. Error bars denote SEM. (d) Changes in connectivity between the SFG.R and the PostCG.R, PostCG.L, PreCG.R after treatment were positively correlated with alterations in Tsui score. Dashed line indicates 95% confidence interval [Colour figure can be viewed at wileyonlinelibrary.com]

CONFLICT OF INTEREST

None.

AUTHOR CONTRIBUTIONS

Liang Feng and Dazhi Yin: conception and design, data analysis, interpretation of results, manuscript draft. Xiangbin Wang and Yongsheng Xiang: imaging data acquisition. Yifei Xu, Fei Teng and Junhui Su: clinical data acquisition. Yougui Pan and Xiaolong Zhang: botulinum toxin injection treatment. Zheng Wang and Lingjing Jin: conception, design and supervision
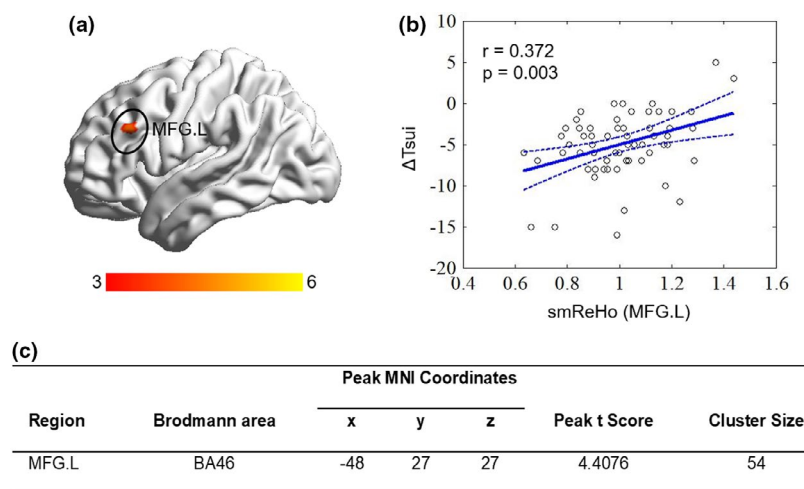
FIGURE 4 Preoperative regional homogeneity of the left middle frontal gyrus predicts clinical response to botulinum toxin type A. (a), (c) Multiple regression analysis between voxel-wise regional homogeneity (smReHo) and changes in Tsui score in 62 patients with cervical dystonia showed that preoperative smReHo of the left middle frontal gyrus (MFG.L) predicted clinical response to treatment. Age, sex, education, mean head motion and disease duration were included as covariates ($p < 0.05$, AlphaSim corrected with voxel-level $p < 0.001$). Warm color denotes positive association, and the color bar indicates t values. (b) Pearson correlation analysis showed a significant positive relationship between baseline smReHo of left MFG and changes in Tsui score in 62 patients. Dashed line indicates 95% confidence interval [Colour figure can be viewed at wileyonlinelibrary.com]

of the project. All authors were responsible for manuscript revision.

DATA AVAILABILITY STATEMENT

The data that support the findings of this study are available on request from the corresponding author. The data are not publicly available due to privacy or ethical restrictions. Data not shown or raw data for analysis will be shared in an anonymized and numerical way on request from any qualified investigator.

ORCID

Lingjing Jin ![ORCID] https://orcid.org/0000-0001-7199-2578

REFERENCES

1. Defazio G, Abbruzzese G, Livrea P, Berardelli A. Epidemiology of primary dystonia. *Lancet Neurol*. 2004;3:673-678.
2. Albanese A, Bhatia K, Bressman SB, et al. Phenomenology and classification of dystonia: a consensus update. *Mov Disord*. 2013;28:863-873.
3. Colosimo C, Suppa A, Fabbrini G, et al. Craniocervical dystonia: clinical and pathophysiological features. *Eur J Neurol*. 2010;17(Suppl 1):15-21.
4. Velickovic M, Benabou R, Brin MF. Cervical dystonia pathophysiology and treatment options. *Drugs*. 2001;61:1921-1943.
5. Neychev VK, Fan XL, Mitev VI, et al. The basal ganglia and cerebellum interact in the expression of dystonic movement. *Brain*. 2008;131:2499-2509.
6. Corp DT, Joutsa J, Darby RR, et al. Network localization of cervical dystonia based on causal brain lesions. *Brain*. 2019;142:1660-1674.
7. Obermann M, Vollrath C, De Greiff A, et al. Sensory disinhibition on passive movement in cervical dystonia. *Mov Disord*. 2010;25:2627-2633.
8. Naumann M, Magyar-Lehmann S, Reiners K, et al. Sensory tricks in cervical dystonia: perceptual dysbalance of parietal cortex modulates frontal motor programming. *Ann Neurol*. 2000;47:322-328.
9. Shaikh AG, Zee DS, Crawford Douglas J, Jinnah HA. Cervical dystonia: a neural integrator disorder. *Brain*. 2016;139:2590-2599.
10. Jiang W, Lei Y, Wei J, et al. Alterations of interhemispheric functional connectivity and degree centrality in cervical dystonia: a resting-state fMRI study. *Neural Plast*. 2019;2019:7349894.
11. Delnooz CCS, Pasman JW, Beckmann CF, Van de Warrenburg BPC. Task-free functional MRI in cervical dystonia reveals multi-network changes that partially normalize with botulinum toxin. *PLoS One*. 2013;8:e62877.
12. Delnooz CCS, Pasman JW, Beckmann CF, Van de Warrenburg BPC. Altered striatal and pallidal connectivity in cervical dystonia. *Brain Struct Funct*. 2015;220:513-523.
13. Conte A, Rocchi L, Latorre A, et al. Ten-year reflections on the neurophysiological abnormalities of focal dystonias in humans. *Mov Disord*. 2019;34:1616-1628.
14. Richardson SP, Tinaz S, Chen R. Repetitive transcranial magnetic stimulation in cervical dystonia: effect of site and repetition in a randomized pilot trial. *PLoS One*. 2015;10:e0124937.
15. Rodrigues FB, Duarte GS, Prescott D, et al. Deep brain stimulation for dystonia. *Cochrane Database Syst Rev*. 2019;1:CD012405.
16. Sarasso E, Agosta F, Piramide N, et al. Sensory trick phenomenon in cervical dystonia: a functional MRI study. *J Neurol*. 2020;267:1103-1115.
17. Simpson DM, Blitzer A, Brashear A, et al. Assessment: Botulinum neurotoxin for the treatment of movement disorders (an evidence-based review): report of the therapeutics and technology assessment subcommittee of the American Academy of Neurology. *Neurology*. 2008;70:1699-1706.
18. Weise D, Weise CM, Naumann M. Central effects of botulinum neurotoxin—evidence from human studies. *Toxins (Basel)*. 2019;11(1):21.
19. Opavský R, Hlustik P, Otruba P, Kanovsky P. Somatosensory cortical activation in cervical dystonia and its modulation with botulinum toxin: an fMRI study. *Int J Neurosci*. 2012;122:45-52.

20. Nevrly M, Hlustik P, Hok P, et al. Changes in sensorimotor network activation after botulinum toxin type A injections in patients with cervical dystonia: a functional MRI study. *Exp Brain Res.* 2018;236:2627-2637.

21. Opavský R, Hlustik P, Otruba P, Kanovsky P. Sensorimotor network in cervical dystonia and the effect of botulinum toxin treatment: a functional MRI study. *J Neurol Sci.* 2011;306:71-75.

22. Brodoehl S, Wagner F, Prell T, et al. Cause or effect: altered brain and network activity in cervical dystonia is partially normalized by botulinum toxin treatment. *Neuroimage Clin.* 2019;22:101792.

23. Hallett M. Mechanism of action of botulinum neurotoxin: unexpected consequences. *Toxicon.* 2018;147:73-76.

24. Feng L, Zhang ZY, Issa MD, et al. The efficacy of single-photon emission computed tomography in identifying dystonic muscles in cervical dystonia. *Nucl Med Commun.* 2020;41:651-658.

25. Zhan Y, Wei J, Liang J, et al. Diagnostic classification for human autism and obsessive–compulsive disorder based on machine learning from a primate genetic model. *Am J Psychiatry.* 2021;178:65-76.

26. Cai DC, Wang Z, Bo T, et al. MECP2 duplication causes aberrant GABA pathways, circuits and behaviors in transgenic monkeys: neural mappings to patients with autism. *J Neurosci.* 2020;40:3799-3814.

27. Yin D, Liu W, Zeljic K, et al. Dissociable changes of frontal and parietal cortices in inherent functional flexibility across the human life span. *J Neurosci.* 2016;36:10060-10074.

28. Anticevic A, Brumbaugh MS, Winkler AM, et al. Global prefrontal and fronto-amygdala dysconnectivity in bipolar I disorder with psychosis history. *Biol Psychiatry.* 2013;73:565-573.

29. Yin D, Luo Y, Song F, et al. Functional reorganization associated with outcome in hand function after stroke revealed by regional homogeneity. *Neuroradiology.* 2013;55:761-770.

30. Obermann M, Yaldizli O, De Greiff A, et al. Increased basal-ganglia activation performing a non-dystonia-related task in focal dystonia. *Eur J Neurol.* 2008;15:831-838.

31. Berman BD, Honce JM, Shelton E, et al. Isolated focal dystonia phenotypes are associated with distinct patterns of altered microstructure. *Neuroimage Clin.* 2018;19:805-812.

32. Fabbrini G, Pantano P, Totaro P, et al. Diffusion tensor imaging in patients with primary cervical dystonia and in patients with blepharospasm. *Eur J Neurol.* 2008;15:185-189.

33. Conte A, Defazio G, Hallett M, et al. The role of sensory information in the pathophysiology of focal dystonias. *Nat Rev Neurol.* 2019;15:224-233.

34. Burciu RG, Hess CW, Coombes SA, et al. Functional activity of the sensorimotor cortex and cerebellum relates to cervical dystonia symptoms. *Hum Brain Mapp.* 2017;38:4563-4573.

35. Li Z, Prudente CN, Stilla R, et al. Alterations of resting-state fMRI measurements in individuals with cervical dystonia. *Hum Brain Mapp.* 2017;38:4098-4108.

36. Prudente CN, Stilla R, Singh S, et al. A functional magnetic resonance imaging study of head movements in cervical dystonia. *Front Neurol.* 2016;7:201.

37. Quartarone A, Hallett M. Emerging concepts in the physiological basis of dystonia. *Mov Disord.* 2013;28:958-967.

38. Neychev VK, Gross RE, Lehericy S, et al. The functional neuroanatomy of dystonia. *Neurobiol Dis.* 2011;42:185-201.

39. Yin D, Zhang C, Lv Q, et al. Dissociable frontostriatal connectivity: mechanism and predictor of the clinical efficacy of capsulotomy in obsessive–compulsive disorder. *Biol Psychiatry.* 2018;84:926-936.

40. Filip P, Gallea C, Lehericy S, et al. Disruption in cerebellar and basal ganglia networks during a visuospatial task in cervical dystonia. *Mov Disord.* 2017;32:757-768.

SUPPORTING INFORMATION

Additional supporting information may be found online in the Supporting Information section.